Effect of Nonlocal Elasticity and Phase Lags on the Magneto Thermoelastic Waves in a Composite Cylinder with Hall Current

Rajendran Selvamani[1,*], S. Mahesh[2] and Farzad Ebrahimi[3]

[1]*Department of Mathematics, Karunya Institute of Technology and Sciences, Coimbatore, India*
[2]*Department of Mathematics, V.S.B. Engineering College, Karur, India-639111*
[3]*Department of Mechanical Engineering, Imam Khomeini International University, Qazvin, Iran*
E-mail: selvam1729@gmail.com; maheshfuzzy1@gmail.com
[*]*Corresponding Author*

Received 26 September 2022; Accepted 09 June 2023;
Publication 11 July 2023

Abstract

In this study, the effect of nonlocal scale value and two phases lags on the free vibration of generalized magneto thermoelastic multilayered LEMV (Linear Elastic Material with Voids)/CFRP (Carbon Fiber Reinforced Polymer) composite cylinder is studied using nonlocal form of linear theory of elasticity. The governing equation of motion is established in longitudinal axis and variable separation model is used to transform the governing equations into a system of differential equations. To investigate vibration analysis from frequency equations, the stress free boundary conditions are adopted at the inner, outer and interface boundaries. The graphical representation of the numerically calculated results for frequency shift, natural frequency, and

European Journal of Computational Mechanics, Vol. 32_2, 157–182.
doi: 10.13052/ejcm2642-2085.3223
© 2023 River Publishers

thermoelastic damping is presented. A special care has been taken to inspect the effect of nonlocal parameter on the aforementioned quantities. The results suggest that the nonlocal scale and the phase lag parameters alter the vibration characteristics of composite cylinders significantly.

Keywords: Multilayered cylinders, non local, LEMV/CFRP, thermoelastic, phase lags, hall current.

1 Introduction

The anticipated models of nonlocal elasticity and nonlocal thermoelasticity solids be subject to different approaches of additional functions of solid mechanics and go through stress-strain relations, governing equations and laws of equilibrium, were deliberated by [1–6]. Under the precise conditions studied, the response of both models is identical for steady homogeneous flows such as steady simple shear flow or pure extension by [7]. To put the method to the test, some important problems in 2D incompressible elasticity are addressed. It is demonstrated that it can be effectively used to capture large strains of incompressible solids by [8]. A center manifold reduction theorem for quasilinear elliptic equations posed on infinite cylinders that is done without a phase space in the sense that we avoid explicitly reformulating the PDE as an evolution problem, as well as an exact solution for the problem of large deformations of torsion, axial tension–compression, and radial expansion or shrinkage of an elastic hollow circular cylinder equipped with pre-stressed elastic coatings and the effect of preliminary stresses coatings on the stress–strain state of a cylindrical pipe by [9, 10]. New approach opens a new avenue to modeling of soft materials accurately and conveniently at large deformation, directly from the data by [11]. Vibration analysis of multilayered composite LEMV/CFRP cylinders are investigated and the effect of the rotation, initial stress and gravity discussed by [12–15].

Layered shells subjected to static loading are taken into account. The theory is founded on a variational formulation in which the associated Euler-Lagrange equations include, in addition to the usual shell equations formulated in stress resultants, the equilibrium of higher order stress resultants resulting from the thickness integration of the local equilibrium equations by [16]. A rigorous (nonlinear) basic state and asymptotic analysis of buckling of compressed thin cylindrical shells are used and novel singular-perturbation problem that arises as a result of the preceding problems by [17]. The phenomenon of snap-buckling in an infinitely long nanocomposite cylindrical panel subjected to uniformly distributed transverse pressure loading is investigated by [18]. [19] deliberated thermoelastic solutions for thermal distributions moving over thin slim rod under memory-dependent three-phase lag magneto-thermoelasticity and memory response in a magneto-thermoelastic rod with moving heat source based on Eringen's nonlocal theory under dual-phase lag heat conduction. [20] debated three-dimensional thermoelasticity analysis of graphene platelets reinforced cylindrical panel. [22] deliberated nonlocal theory of thermoelastic materials with voids and fractional derivative heat transfer. [23] studied thermoelastic interactions on hyperbolic two-temperature generalized thermoelasticity in an infinite medium with a cylindrical cavity. [24] investigated of thermal preloading and porosity effects on the nonlocal nonlinear instability of FG nanobeams with geometrical imperfection. The combined effect of electric and magnetic field in a conductor is known as hall current due to their properties its more attention. Lata and Singh [25–27] studied the wave propagation in nonlocal magneto-thermoelastic solids with Hall current and discussed the various effects on wave characteristics.

Forced vibration analysis in axisymmetric functionally graded viscothermoelastic hollow cylinder under dynamic pressure and effect of three-phase-lag model on the analysis of three-dimensional free vibrations of viscothermoelastic solid cylinder is discussed by [28–32]. Effect of dual-phase-lag and three phase lag model on the vibration analysis of nonlocal generalized thermoelastic diffusive hollow sphere and hollow sphere with voids is investigated by [33].

In the current work, we originate the new constitutive relations and the governing equations for nonlocal thermoelastic multilayered composite cylinder in the existence of Eringen's nonlocal elasticity model. Variable separation is used to convert the governing equations into a system of differential equations. For traction-free thermal boundary conditions, the frequency equation is investigated for the survival of a variety of possible modes in compact form: thermally insulated and isothermal boundary conditions. To investigate vibration analysis from frequency equations, we use the numerical technique to generate numerical data with the help of the Matlab software. The numerically computed and simulated results for frequency shift, natural frequency, and thermoelastic damping are addressed with graphs and tables.

2 Modelling of Problem

A homogeneous, transversely isotropic elastic cylinder of inner and outer radius x and a exposed with thermal field in axial direction is considered for the free vibration of nonlocal composite cylinder. The displacement with hall current and thermal field equations in cylindrical coordinates (r, z) is given by

$$\sigma^l_{rr,r} + \sigma^l_{rz,z} + r^{-1}(\sigma^l_{rr}) + (1 - \epsilon^2\nabla^2)\vec{F}_r = (1 - \epsilon^2\nabla^2)\rho u^l_{,tt} \tag{1a}$$

$$\sigma^l_{rz,r} + \sigma^l_{zz,z} + r^{-1}\sigma^l_{rz} + (1 - \epsilon^2\nabla^2)\vec{F}_z = (1 - \epsilon^2\nabla^2)\rho w^l_{,tt} \tag{1b}$$

$$K_{11}(T^l_{,rr} + r^{-1}T^l_{,r}) + \tau_t(K_{11}T^l_{,rr} + K_{33}T^l_{,zz})_{,t}$$
$$= \left(\delta + \tau_q\frac{\partial}{\partial t}\right)[T_0 dT^l_{,t} + T_0(\beta_1(e^l_{rr} + e^l_{\theta\theta}) + \beta_3 e^l_{,zz})] \tag{1c}$$

The non-local stress strain relations are given as follows [31]

$$(1 - \epsilon^2\nabla^2)\sigma^l_{rr} = c_{11}e^l_{rr} + c_{12}e^l_{\theta\theta} + c_{13}e^l_{zz} - \beta_1 T^l \tag{2a}$$

$$(1 - \epsilon^2\nabla^2)\sigma^l_{zz} = c_{13}e^l_{rr} + c_{13}e^l_{\theta\theta} + c_{33}e^l_{zz} - \beta_3 T^l \tag{2b}$$

$$(1 - \epsilon^2\nabla^2)\sigma^l_{rz} = c_{44}e^l_{rz} \tag{2c}$$

where $\sigma^l_{rr}, \sigma^l_{r\theta}, \sigma^l_{rz}, \sigma^l_{\theta\theta}, \sigma^l_{zz}, \sigma^l_{\theta z}$ are the stress and $e^l_{rr}, e^l_{zz}, e^l_{\theta\theta}, e^l_{r\theta}, e^l_{z\theta}, e^l_{rz}$ are the strain components, T is the temperature, $c_{11}, c_{12}, c_{13}, c_{33}, c_{44}, c_{66}$ are the elastic moduli, β_1, β_3 are thermal expansion moduli and K_1, K_3 thermal conductivities, ρ is density, c_v is specific heat capacity and τ_θ and τ_q are phase lags. Here $\epsilon = e_0 a_0$ is the elastic nonlocal parameter, a_0 is the internal characteristic length and e_0 is a material constant.

The current density from the $J_x = \frac{\sigma_0\mu_0 H_0}{1+m^2}(mu_{,t} - w_{,t})$ and $J_z = \frac{\sigma_0\mu_0 H_0}{1+m^2}$ $(u_{,t} + mw_{,t})$ can be computed from the Lorentz's force $\vec{F_i} = \mu_0(\vec{J} \times \vec{H}_0)_i$ in which $\vec{j} = \frac{\sigma_0}{1+m^2}(\vec{E} + \mu_o(\vec{u} \times \vec{H} - \frac{1}{en_e}\vec{j} \times \vec{H}_0))$ Lata and Singh [2021].

Where, σ_0 is the electrical conductivity, $m(= \omega_e t_e)$ is the Hall parameter, ω_e is the electronic frequency, t_e is the electron collision time, e is the charge of an electron, ne is the number of density of electrons.

The strains fields of the cylinder is taken as

$$e^l_{rr} = u^l_{,r} e^l_{\theta\theta} = r^{-1}(u^l + v^l_{,\theta}), \quad e^l_{zz} = w^l_{,z}$$

$$e^l_{r\theta} = v^l_r - r^{-1}(v^l - u^l_{,\theta}), \quad e^l_{z\theta} = v^l_{,z} + r^{-1}w^l_{,\theta},$$
$$e^l_{rz} = w^l_{,r} + u^l_{,z} \tag{3}$$

Substitution of the "Equation (3) and (2)" into "Equation (1)" gives the following small motion equations.

$$\frac{c_{11}}{1-\epsilon^2\nabla^2}(u^l_{,rr} + r^{-1}u^l_{,r} + r^{-2}u^l) + \frac{c_{13}}{1-\epsilon^2\nabla^2}w^l_{,rz}$$
$$+ \frac{c_{44}}{1-\epsilon^2\nabla^2}(u^l_{,zz} + w^l_{,rz}) - \frac{\beta^l_1}{(1-\epsilon^2\nabla^2)}T^l_{,r}$$
$$- (1-\epsilon^2\nabla^2)\frac{\mu_0^2 H_0^2\sigma^2}{1+m^2}(u_{,t} + mw_{,t}) = (1-\epsilon^2\nabla^2)\rho^l u_{,tt} \tag{4a}$$

$$\frac{(c_{44}+c_{13})}{1-\epsilon^2\nabla^2}(u^l_{,rz} + r^{-1}u^l_{,z}) + \frac{c_{33}}{1-\epsilon^2\nabla^2}(w^l_{,zz})$$
$$+ \frac{c_{44}}{1-\epsilon^2\nabla^2}(w^l_{,rr} + r^{-1}w^l_{,r}) - \frac{\beta^l_3}{1-\epsilon^2\nabla^2}T^l_{,r}$$
$$- (1-\epsilon^2\nabla^2)\frac{\mu_0^2 H_0^2\sigma^2}{1+m^2}(mu_{,t} - w_{,t}) = (1-\epsilon^2\nabla^2)\rho^l w_{,tt} \tag{4b}$$

$$K_{11}(T^l_{,rr} + r^{-1}T^l_{,r}) + \tau_\theta(K_{11}T^l_{,rr} + K_{33}T^l_{,zz})_{,t}$$
$$= \left(\delta + \tau_q\frac{\partial}{\partial t}\right)[T_0 dT^l_{,t} + T_0(\beta_1(u^l_{,rt} + r^{-1}u^l_{,t}) + \beta_3 w^l_{,z})] \tag{4c}$$

where K_{ij} is heat conduction coefficient, $d = \frac{\rho C_v}{T_0}$. The coupled thermoelasticity (CTE) theory may be obtained when $\tau_\theta = \tau_q = 0$ and $\delta = 1$ in "Equation (4c)". The Lord–Shulman (LS) generalized thermoelasticity theory may be obtained when $\tau_\theta, \tau_q \to 0$, $\delta = 1$ in "Equation (4c)". The Green–Naghdi (GN) thermoelasticity is obtained when $\tau_\theta, \tau_q \to 0, \delta = 0$ in "Equation (4c)".

The time harmonic solutions of "Equation (4)", is assumed as

$$u^l = U^l_{,r}\exp\{i(kz+pt)\}$$
$$w^l = \left(\frac{i}{h}\right)W^l\exp\{i(kz+pt)\}$$
$$T^l = \left(\frac{c_{44}}{\beta_3}\right)\left(\frac{\phi^l}{h^2}\right)\exp\{i(kz+pt)\} \tag{5}$$

Where, u^l, w^l, φ^l indicates the displacement potential function, k is the wave number parameter, p is the angular frequency $i = \sqrt{-1}$. For convenient problem solving, we set the following non-dimensional values $x = \frac{r}{a}, \varepsilon = ka, c = \rho p, \Omega = \frac{\rho p^2 a^2 (1-\epsilon^2\nabla^2)^2}{c_{44}}$

$$\overline{c}_{11} = c_{11}(1-\epsilon^2\nabla^2)/c_{44}, \overline{c}_{13} = c_{13}(1-\epsilon^2\nabla^2)/c_{44},$$

$$\overline{c}_{33} = c_{33}(1-\epsilon^2\nabla^2)/c_{44},\ \overline{c}_{66} = c_{66}(1-\epsilon^2\nabla^2)/c_{44},$$

$$\overline{\beta} = \beta_1(1-\epsilon^2\nabla^2)/\beta_3, \overline{k}_i = \frac{(\rho c_{44})^{\frac{1}{2}}}{\beta_3^2 T_0 a\Omega},\ N = \frac{(1-\epsilon^2\nabla^2)^2}{c_{44}}\frac{\mu_0^2 H_0^2 \sigma^2}{1+m^2}.$$

Substituting “Equation (5)”, in “Equation (4)”, we obtain:

$$[\overline{c}_{11}\nabla^2 - (\Omega^2 - \varepsilon^2) - iNp]U^l - \left[\varepsilon(1+\overline{c}_{13}) + Nm\left(\frac{p}{h}\right)\right]W^l - \overline{\beta}\phi^l = 0$$

$$[\varepsilon(1+\overline{c}_{13})\nabla^2 - imNp]U^l + [\nabla^2 + (\Omega^2 - \overline{c}_{33}\varepsilon^2)] + m\left(\frac{p}{h}\right)]W^l - \varepsilon\phi^l = 0$$

$$\frac{\overline{\beta}T_0 z}{c_{44}}\nabla^2 U^l + \frac{\tau_q p^2 ia}{c_{44}}W^l + \left(\frac{i\overline{K}_{11}}{\overline{\beta}a^2}\nabla^2(1+\tau_t) + \frac{i\overline{K}_{33}}{\overline{\beta}}(1+ip\tau_t)\varepsilon^2 - \frac{\rho\overline{d}ip}{\overline{\beta}}(1-\tau_q)\right)\phi^l = 0 \tag{6}$$

“Equation (6)”, can be written as in the following form using above relations

$$\begin{vmatrix} [\overline{c}_{11}\nabla^2 - (\Omega^2-\varepsilon^2) - iNp] & \left[\varepsilon\left(1+\overline{c}_{13}\right) + Nm\left(\frac{p}{h}\right)\right] & \overline{\beta} \\ [\varepsilon(1+\overline{c}_{13})\nabla^2 - imNp] & \left[\nabla^2 + (\Omega^2 - \overline{c}_{33}\varepsilon^2) + m\left(\frac{p}{h}\right)\right] & \varepsilon \\ \frac{\overline{\beta}T_0 z}{c_{44}}\nabla^2 & \frac{\tau_q p^2 ia}{c_{44}} & \left(\frac{i\overline{K}_{11}}{\overline{\beta}a^2}\nabla^2(1+\tau_t) + H\right) \end{vmatrix} \times (U^l\ W^l\ \phi^l)^T = 0 \tag{7}$$

Bifurcating the “Equation (7)”, we can arrive

$$(A\nabla^6 + B\nabla^4 + C\nabla^2 + D)(U^l\ W^l\ \phi^l)^T = 0 \tag{8}$$

where

$$A = \bar{c}_{11}\frac{i\overline{K}_{11}}{\overline{\beta}a^2}(1+\tau_t)$$

$$B = \bar{c}_{11}H + \bar{c}_{11}\frac{i\overline{K}_{11}}{\overline{\beta}a^2}(1+\tau_t)\left(\Omega^2 - \bar{c}_{33}\varepsilon^2 + m\left(\frac{p}{h}\right)\right)$$

$$- (\Omega^2 - \varepsilon^2 - iNp)\frac{i\overline{K}_{11}}{\overline{\beta}a^2}(1+\tau_t)$$

$$+ [\varepsilon^2(1+\bar{c}_{13}) + \varepsilon(1+\bar{c}_{13})]\frac{i\overline{K}_{11}}{\overline{\beta}a^2}(1+\tau_t) - \frac{\overline{\beta}^2 T_0 z}{c_{44}}$$

$$C = \bar{c}_{11}(\Omega^2 - \bar{c}_{33}\varepsilon^2 +)H - \bar{c}_{11}\varepsilon^2\frac{\tau_q p^2 ia}{c_{44}} - (\Omega^2 - \varepsilon^2)H$$

$$- (\Omega^2 - \varepsilon^2)\frac{i\overline{K}_{11}}{\overline{\beta}a^2}(1+\tau_t)\left(\Omega^2 - \bar{c}_{33}\varepsilon^2 + m\left(\frac{p}{h}\right)\right)$$

$$+ [H\varepsilon^2(1+\bar{c}_{13}) - imNp] - [imNp + (1+\bar{c}_{13})\varepsilon^2]\frac{\overline{\beta}T_0 z}{c_{44}}$$

$$+ \overline{\beta}[imNp(1+\bar{c}_{13})\varepsilon^2]\frac{\tau_q p^2 ia}{c_{44}} - \left(\Omega^2 - \bar{c}_{33}\varepsilon^2 + m\left(\frac{p}{h}\right)\right)\frac{\overline{\beta}^2 T_0 z}{c_{44}}$$

$$D = \varepsilon[(\Omega^2 - \varepsilon^2) - iNp]\frac{\tau_q p^2 ia}{c_{44}}$$

$$- (\Omega^2 - \varepsilon^2 - iNp)\left(\Omega^2 - \bar{c}_{33}\varepsilon^2 + m\left(\frac{p}{h}\right)\right)H$$

$$H = \frac{i\overline{K}_{33}}{\overline{\beta}}(1 + ip\tau_t)\varepsilon^2 - \frac{\rho\bar{d}ip}{\overline{\beta}}(1-\tau_q)$$

When the relationship given in “Equation (8)”, is factored into a biquadratic equation for $(\alpha_j^l a)^2$, j = 1, 2, 3, 4 and the symmetric mode solutions are derived as

$$U^l = \sum_{j=1}^{3}[A_j J_n(\alpha_j x) + B_j y_n(\alpha_j x)],$$

$$W^l = \sum_{j=1}^{3} a_j^l [A_j J_n(\alpha_j x) + B_j y_n(\alpha_j x)],$$

$$\phi^l = \sum_{j=1}^{3} b_j^l [A_j J_n(\alpha_j x) + B_j y_n(\alpha_j x)], \tag{9}$$

Where $(\alpha_j^l ax) > 0$, for $(j = 1, 2, 3, 4)$ are the zeros the following equation

$$(A(\alpha_j^l a)^6 + B(\alpha_j^l a)^4 + C(\alpha_j^l a)^2 + D)(U^l\ W^l\ \phi^l)^T = 0 \tag{10}$$

The following relations ensure the values of the constants a_j^l, b_j^l and c_j^l in "Equation (9)".

$$[\bar{c}_{11}\nabla^2 - (\Omega^2 - \varepsilon^2) - iNp] - [\varepsilon(1 + \bar{c}_{13})]a_j^l - \overline{\beta}b^l{}_j = 0$$

$$[\varepsilon(1 + \bar{c}_{13})\nabla^2] + \left[\nabla^2 + \left(\Omega^2 - \bar{c}_{33}\varepsilon^2 + m\left(\frac{p}{h}\right)\right) H\right] a_j^l - \varepsilon b_j^l = 0$$

$$\overline{\beta}\nabla^2 + \varepsilon a_j^l + (i\overline{K}_1\nabla^2 + i\overline{K}_3\varepsilon^2 - \overline{d} + \overline{H})b^l{}_j = 0$$

3 Motion Model for Linear Elastic Materials with Voids (LEMV)

The motion equation of displacement and equilibrated inertia of LEMV is modelled as

$$\begin{aligned}
&(\lambda + 2\mu)(u_{,rr} + r^{-1}u_{,r} - r^{-2}u) + \mu u_{,zz} \\
&\qquad + (\lambda + \mu)w_{,zz} + \beta\psi_{,r} = \rho u_{tt} \\
&(\lambda + \mu)(u_{,rz} + r^{-1}u_{,z}) + \mu(w_{,rr} + r^{-1}w_{,r}) \\
&\qquad + (\lambda + 2\mu)w_{,zz} + \beta\psi_{,z} = \rho w_{,tt} \\
&- \beta(u_{,r} + r^{-1}u) - \beta w_{,z} + \alpha(\psi_{,rr} + r^{-1}\psi_{,r} + \psi_{,zz}) \\
&\qquad - \delta k\psi_{,tt} - \omega\psi_{,t} - \xi\psi = 0
\end{aligned} \tag{11}$$

The LEMV stress is given as

$$\sigma_{,rr} = (\lambda + 2\mu)u_{,r} + \lambda r^{-1}u + \lambda w_{,z} + \beta\phi$$

$$\sigma_{rz} = \mu(u_{,t} + w_{,r}).$$

The solution of "Equation (11)", is considered as

$$u = U_{,r} expi(kz + pt)$$
$$w = \left(\frac{i}{h}\right) W expi(kz + pt)$$
$$\psi = \left(\frac{1}{h^2}\right) \chi \, expi(kz + pt) \tag{12}$$

"Equation (11)", can be reduced in the following determinant form for further estimation

$$\begin{vmatrix} (\lambda + 2\mu)\nabla^2 + k_1 & -k_2 & k_3 \\ k_2\nabla^2 & \overline{\mu}\nabla^2 + k_4 & k_5 \\ -k_3\nabla^2 & k_5 & \alpha\nabla^2 + k_6 \end{vmatrix} (U, W, \chi) = 0 \tag{13}$$

Where

$$\nabla^2 = \frac{\partial^2}{\partial x^2} + \frac{1}{x}\frac{\partial}{\partial x}$$
$$k_1 = (ch)^2 \frac{\rho}{\rho^1} - \varepsilon^2 \overline{\mu}, \; k_2 = (\overline{\lambda} + \overline{\mu})\varepsilon, \; k_3 = \overline{\beta},$$
$$k_4 = (ch)^2 \frac{\rho}{\rho^1} - \varepsilon^2 (\overline{\lambda} + \overline{\mu}), \; k_5 = \overline{\beta}\varepsilon$$
$$k_6 = \frac{\rho}{\rho^1}(ch)^2 \overline{k} - \overline{\alpha}\varepsilon^2 - i\overline{\omega}(ch) - \overline{\xi}$$

The "Equation (13)", can be rewritten as,

$$(\nabla^6 + P_{11}\nabla^4 + P_{12}\nabla^2 + P_{13})(U, W, \psi) = 0 \tag{14}$$

Where

$$P_{11} = \frac{[(\overline{\lambda} + 2\overline{\mu})k_6\overline{\mu} + (\overline{\lambda} + 2\overline{\mu})\alpha k_4 + k_1\alpha\overline{\mu} + k_2^2\alpha + k_3^2\overline{\mu}]}{(\overline{\lambda} + 2\overline{\mu})\alpha\overline{\mu}}$$
$$P_{12} = \frac{\begin{array}{c}[(\overline{\lambda} + 2\overline{\mu})k_4k_6 + (\overline{\lambda} + 2\overline{\mu})k_5^2 + k_1k_6\overline{\mu} \\ + k_4k_1\alpha + k_2^2S_6 + 2k_2k_3k_5 + k_3^2k_4]\end{array}}{(\overline{\lambda} + 2\overline{\mu})\alpha\overline{\mu}}$$
$$P_{13} = \frac{k_1k_4k_6 - k_1k_5^2}{(\overline{\lambda} + 2\overline{\mu})\alpha\overline{\mu}}$$

The solution of “Equation (14)”, is estimated as

$$U = \sum_{j=1}^{3} [A_j J_0(\alpha_j x) + B_j y_0(\alpha_j x)],$$

$$W = \sum_{j=1}^{3} a_j [A_j J_0(\alpha_j x) + B_j y_0(\alpha_j x)],$$

$$\chi = \sum_{j=1}^{3} b_j [A_j J_0(\alpha_j x) + B_j y_0(\alpha_j x)],$$

The values of a_j and b_j are calculated from the following relations

$$k_2 \nabla^2 + (\overline{\mu} \nabla^2 + k_4) a_j + k_5 b_j = 0,$$
$$-k_3 \nabla^2 + k_5 a_j + (\alpha \nabla^2 + k_6) b_j = 0$$

4 Boundary Conditions-Frequency Equations

In order to get the required dispersion relation, the following boundary conditions are adopted along inner, outer and interface area of nonlocal composite cylinder.

(i) $\sigma^l_{rr} = \sigma^l_{rz} = T^l = 0$ with $l = 1, 3$
(ii) $\sigma^l_{rr} = \sigma_{rr}; \sigma^l_{rz} = \sigma_{rz}; T^l = 0;$

A 18 $\times$ 18 determinant is reached while plugging the above boundary conditions in the obtained solutions

$$|(R_{ij})| = 0, \ (i, j = 1, 2, 3, \ldots 18) \tag{15}$$

At $x = x_0$ Where $j = 1, 2, 3$

$$R_{1j} = 2\overline{c}_{66} \left(\frac{\alpha^1_j}{x_0} \right) J_1(\alpha^1{}_j x_0) - [(\alpha^1{}_j a)^2 \overline{c}_{11} + \zeta \overline{c}_{13} a^l{}_j + \overline{\beta} b^l{}_j] J_0(\alpha^1{}_j a x_0)$$

$$R_{2j} = (\zeta + a^1_j + \overline{\beta} b^1_j)(\alpha^1_j) \ J_1(\alpha^1{}_j x_0)$$

$$R_{3j} = \frac{b^1_j}{x_0} J_0(\alpha^1{}_j x_0) - (\alpha^1_j) \ J_1(\alpha^1{}_j x_0)$$

And the other nonzero elements $R_{1,j+4},\ R_{2,j+4}, R_{3,j+4}$ and $R_{4,j+4}$ are obtained by replacing J_0 by J_1 and y_0 by y_1.

At $x = x_1$

$$R_{4j} = 2\overline{c}_{66}\left(\frac{\alpha_j^1}{x_1}\right)J_1({\alpha^1}_j x_1)$$

$$- [({\alpha^1}_j a)^2\overline{c}_{11} + \zeta\overline{c}_{13}{a^l}_j + \overline{\beta}{b^l}_j]J_0({\alpha^1}_j a x_1)$$

$$R_{4,j+8} = -\left[2\overline{\mu}\left(\frac{\alpha_j}{x_1}\right)J_1(\alpha x_1)\right.$$

$$+ \{-(\overline{\lambda}+\overline{\mu})(\alpha_j)^2 + \overline{\beta}b_j - \overline{\lambda}\zeta a_j\}J_0(\alpha_j x_1)$$

$$R_{5j} = (\zeta + a_j^1 + \overline{\beta}b_j^1)(\alpha_j^1)\ J_1({\alpha^1}_j a x_1)$$

$$R_{5,j+8} = -\overline{\mu}(\zeta + a_j)(\alpha_j)J_1(\alpha_j x_1)$$

$$R_{6j} = (\alpha_j^l)J_1(\alpha_j^l x_1)$$

$$R_{6,j+8} = -(\alpha_j)J_1({\alpha^l}_j x_1)$$

$$R_{7j} = a_j^l J_0(\alpha_j^l x_1)$$

$$R_{7,j+8} = -a_j^l J_0(\alpha_j^l x_1)$$

$$R_{8j} = b_j^l J_0(\alpha_j^l x_0)$$

$$R_{8j} = a_j(\alpha_j)J_1(\alpha_j^1 x_1)$$

$$R_{9j} = \frac{b_j^l}{x_1}J_0(\alpha_j^l x_1) - (\alpha_j^l)J_1(\alpha_j^l x_1)$$

And $R_{i,j+4}, R_{i,j+8}, R_{i,j+11}, R_{i,j+14},\ (i = 5,6,7,8,9)$ and $R_{9,j+4}$, $R_{10,j+4}$, $R_{11,j+4}$, at $x = x_1$ is computed by swapping J_0 by J_1 and y_0 by y_1 in the proceeding values. The values R_{ij}, $(i = 12, 13, \ldots, 15$ and $j = 8, 9, \ldots, 18)$ are drafted by changing x_1 by x_2 at x $= x_2$. Also, the values R_{ij}, $(i = 16, 17, 18$ and $j = 14, 15, \ldots, 18)$ can be derived at x $= x_3$ by proper replacements.

5 Validation of the Results

5.1 Thermal Hollow Cylinder by Multi-dual Phase-lag Theory

From this model, if we ignore the nonlocal parameter ($\in = 0$) and LEMV, we can obtain the vibration of thermal hollow cylinder via a multi-dual phase-lag theory as discussed in [34].

5.2 Pyrocomposite Hollow Cylinder

From this model, if we ignore nonlocal parameter ($\in = 0$) and vanish the parameters phase-lag of the heat flux τ_θ, phase-lag of temperature gradient τ_q and put $\delta = 1$, we can deduce this result in to pyrocomposite hollow cylinderwhich is consistent with the analytical model derived in [35].

5.3 Pyrocomposite Hollow Cylinder with CFRP Core

If the constants like, void volume fraction $\psi = 0$, and the Lame's constants $\lambda = c_{12}, \mu = \frac{c_{11}-c_{12}}{2}$ in the Equation (11), then the analytical model has been reduced in to free vibration analysis of multilayered composite cylinder with embedding core material CFRP.

6 Numerical Discussion

In this subsection, numerical examples are projected to authenticate the proposed analytical model. Also, different theories of thermoelasticity like GTE (generalized thermoelasticity), CTE(coupled thermoelasticity) and E(elasticity) are drafted and studied numerically. The physical constants of CdSe is taken for numerical computation as follows [15]

$$C_{11} = 7.41 \times 10^{10}\ \mathrm{Nm}^{-2};\ C_{12} = 4.52 \times 10^{10}\ \mathrm{Nm}^{-2};$$

$$C_{13} = 3.93 \times 10^{10}\ \mathrm{Nm}^{-2}; C_{33} = 8.36 \times 10^{10}\ \mathrm{Nm}^{-2};$$

$$C_{44} = 1.32 \times 10^{10}\ \mathrm{Nm}^{-2};\ \beta_1 = 0.621 \times 10^{6}\ \mathrm{NK}^{-1}\mathrm{m}^{-2};$$

$$\beta_3 = 0.551 \times 10^{6}\ \mathrm{NK}^{-1}\mathrm{m}^{-2}; \rho = 5504\ \mathrm{kgm}^{-3}; T_0 = 298\ \mathrm{K}$$

The numerically computed complex frequency might be written as $\Omega = \Omega_R + i\Omega_I$, the size dependent frequency shift is defined as

$$\Omega_{Shift} = \frac{|\Omega_R - \Omega_0|}{\Omega_0},$$

Where Ω_R is the real part and Ω_0 is the fundamental vibration frequency of nonlocal polygonal plate in the absence of thermal field and is defined as

$$\Omega_0 = \lambda\sqrt{\frac{E}{\rho(1+\xi^2\lambda^2)}}$$

The thermo elastic damping is taken as

$$Q^{-1} = 2\left|\frac{\Omega_I}{\Omega_R}\right|$$

Numerical results which are obtained for various thermoelasticity theories and nonlocal parameter (ϵ) as function of wave number is derived for multi-layered composite LEMV/CFRP cylinders. The non-dimensional frequency is tested over wave number for various thermo elasticity theories and increasing value of nonlocal parameter (ϵ) are compared in Tables 1 and 2. From this results the influences of various thermoelasticity and nonlocal parameter (ϵ) in non-dimensional frequency is having considerable impact. Especially the nonlocal parameter gives noticeable impact in both LEMV and CFRP cylinders.

Table 1 Non-dimensional frequency in CFRP composite cylinder

	Non-dimensional Frequency					
	Non-Local Parameter $\in= 0.01$			Non-Local Parameter $\in= 0.02$		
Wave Number	CTE	LS	GN	CTE	LS	GN
0.2	0.1455	0.1578	0.1678	0.1549	0.1678	0.1748
0.4	0.2235	0.2458	0.2685	0.2694	0.2874	0.2978
0.6	0.4578	0.5014	0.5874	0.3564	0.3674	0.3874
0.8	0.6547	0.7452	0.8974	0.6878	0.7478	0.8589
1	0.8978	0.9582	1.0258	0.8074	0.9578	1.0010

Table 2 Non-dimensional frequency in LEMV composite cylinder

	Non-dimensional Frequency					
	Non-Local Parameter $\in= 0.01$			Non-Local Parameter $\in= 0.02$		
Wave Number	CTE	LS	GN	CTE	LS	GN
0.2	0.7456	0.8549	1.0214	0.7248	0.7154	0.6985
0.4	0.9885	0.9912	1.1258	0.9568	0.9258	0.9021
0.6	1.0625	1.1258	1.2574	1.002	0.9985	0.9754
0.8	1.4589	1.5421	1.6254	1.2356	1.1125	1.0025
1	1.7895	1.8126	1.8578	1.5684	1.4985	1.3254

Table 3 Variation of Radial, Axial and Temperature in LEMV composite cylinder with $\in = 0.01$

Wave number		CTE	LS	GN
0.2	U	1.2214	1.1422	1.0419
	W	0.8456	0.8248	0.8085
	T	4.1584	4.0587	4.0276
0.4	U	1.5640	1.4599	1.3615
	W	0.8885	0.8568	0.8365
	T	3.2334	3.0572	3.5918
0.6	U	2.1917	2.0865	2.9986
	W	1.0025	1.0020	0.9996
	T	2.6083	2.5357	2.4631
0.8	U	2.6309	2.4622	2.2066
	W	1.2589	1.2356	1.0235
	T	1.2049	1.1242	1.0428
1	U	3.4837	3.2911	3.0588
	W	1.6895	1.5684	1.3258
	T	0.9863	0.656	0.5844

In Tables 3 and 4 the Radial, Axial and Temperature Distribution are observed for multi-layered composite LEMV/CFRP cylinders for amplified wave number values in the presence of various thermoelascity theories and nonlocal parameter. As visualized from these tables, the radial and axial values reaches higher mode as wave number rises. However, this trend is reversed or temperature distribution in both LEMV and CFRP cylinders. Also, a significant effect of various thermo elastic and nonlocal values prevail for all the physical variables.

Variation of non-dimensional frequency against mode number is observed from Figures: 1 & 2 in the presence of various thermoelasticity theories and elasticity for thermoelastic hollow multi-layered LEMV cylinders with the nonlocal and hall current parameters $\in = 0, \in = 0.03$ and $m = 0, m = 0.1$. In all cases for increasing value of mode number (n) frequency keeps linear nature in GTE, CTE for $\in = 0$ & $\in = 0.03$, but in the presence of elasticity (E) and non-local parameter ($\in$) frequency makes light variation from the linear nature.

The non-dimensional frequency as a function of mode number of multi-layered CFRP cylinders are plotted in Figures: 3 & 4 in the presence of various thermoelasticity theories and elasticity with the nonlocal and hall current parameters $\in = 0$, $\in = 0.03$ and $m = 0, m = 0.1$. In Figure 3 the increasing values of mode number frequency values increases in presence the

Table 4 Variation of radial, axial and Temperature in LEMV composite cylinder with $\in= 0.02$

Wave number		CTE	LS	GN
0.2	U	3.4561	3.3589	3.2145
	W	0.8485	0.8258	0.8014
	T	4.3255	4.2589	4.2147
0.4	U	3.7589	3.6587	3.5687
	W	1.0045	1.0005	0.9756
	T	3.4589	3.2147	3.1459
0.6	U	4.3684	4.2457	4.1257
	W	1.1568	1.1025	1.0135
	T	2.8569	2.7489	2.6589
0.8	U	4.8547	4.6859	4.4258
	W	1.4589	1.3589	1.1359
	T	2.4589	2.3258	2.2548
1	U	5.6895	5.4587	5.2589
	W	1.6578	1.5895	1.2689
	T	1.8589	1.7256	1.5896

Table 5 Comparison of dimensionless frequency against wave number with [35]

	Non-dimensional Frequency	
Wave Number	[35]	Present Study
0.2	0.1999	0.1987
0.4	0.6000	0.6056
0.6	0.1200	0.1190
0.8	0.1800	0.1792
1	0.2400	0.2412

Table 6 Comparison of temperature distribution with [34]

	Thermoelasticity Theories	[34]	Present Study
Temperature distribution	CTE	0.557632	0.549321
	L-S	0.469378	0.468198
	G-N	0.254464	0.249533

of GTE, CTE, elasticity (E) for $\in= 0$ & $\in= 0.03$ on the other hand from Figure 4 it can be seen that the presence of GTE, CTE,elasticity (E) and nonlocal parameter frequency keeps tiny oscillation nature increasing values of mode number.

Further, the impact of frequency shift on the mode number of multi-layered LEMV cylinder is observed in Figures 5 and 6 in the presence of

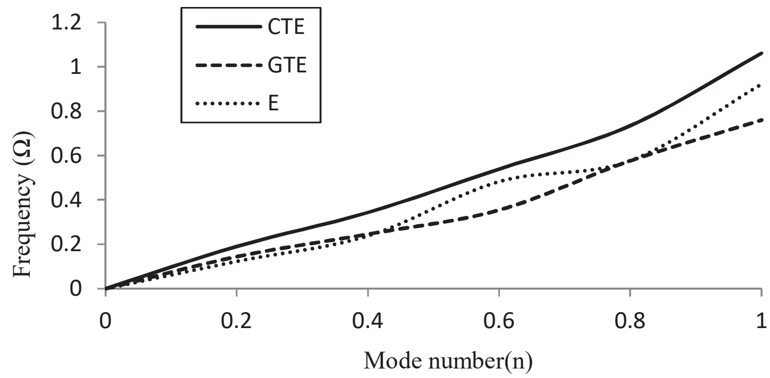

Figure 1 Variation of non-dimensional frequency against mode number (n) in the LEMV cylinder with $\in = 0.03$ & $m = 0.1$.

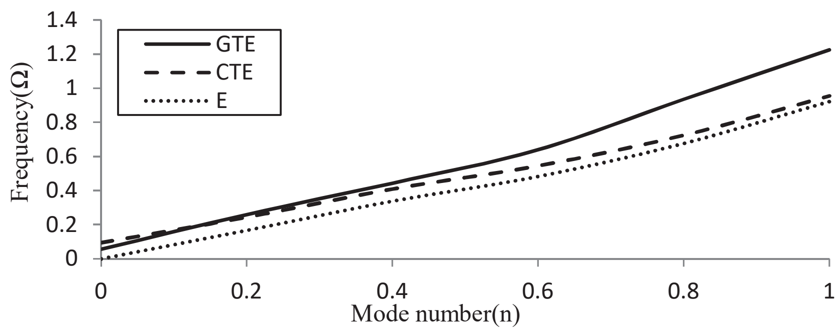

Figure 2 Variation of non-dimensional frequency against mode number (n) in the LEMV cylinder with $\in = 0$ & $m = 0$.

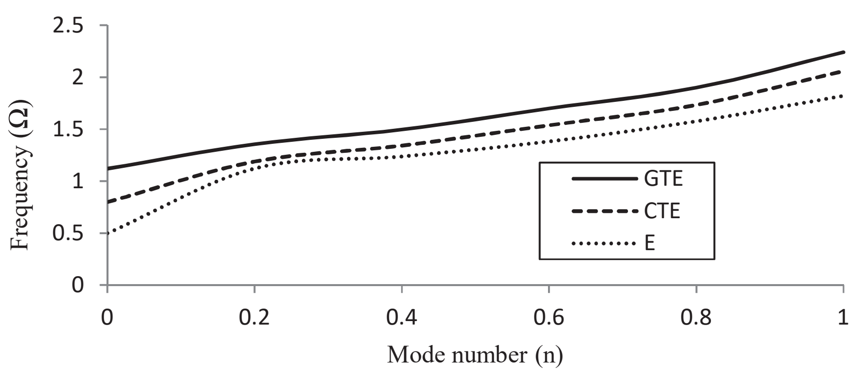

Figure 3 Variation of non-dimensional frequency against mode number (n) in the CFRP cylinder with $\in = 0.03$ & $m = 0.1$.

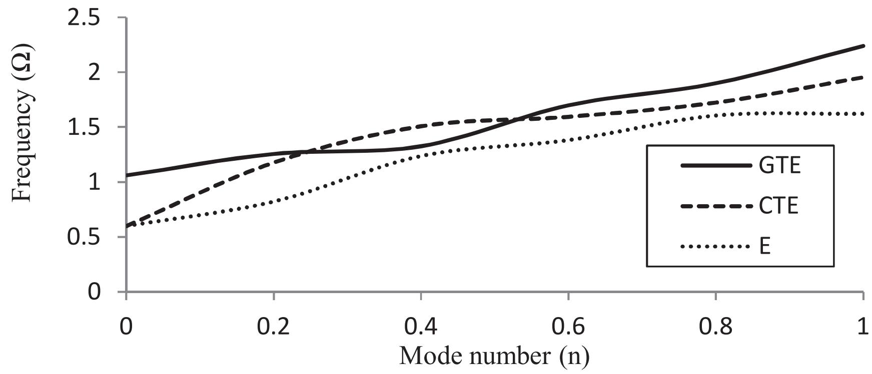

Figure 4 Variation of non-dimensional frequency against mode number (n) in the CFRP cylinder with $\in = 0$ & $m = 0$.

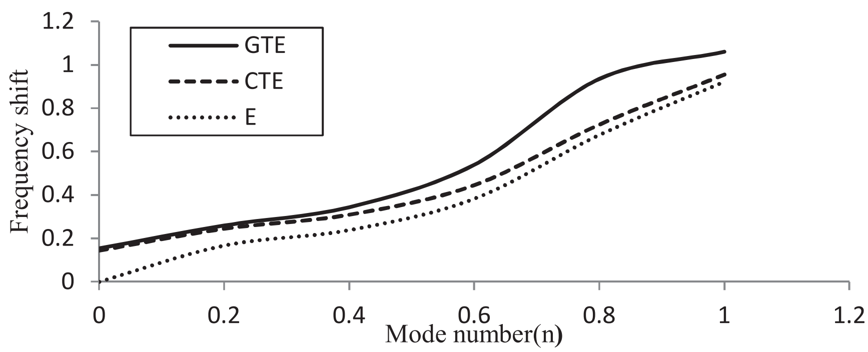

Figure 5 Variation of frequency shift against mode number (n) in the for LEMV cylinder with $\in = 0.03$ & $m = 0.1$.

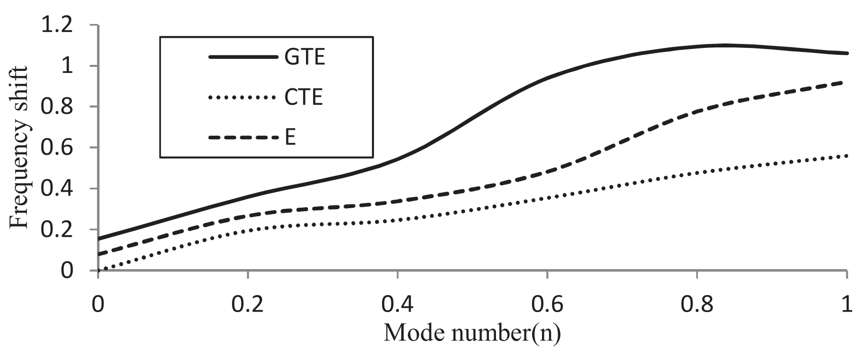

Figure 6 Variation of frequency shift against mode number (n) in the LEMV cylinder with $\in = 0$ & $m = 0$.

various thermoelasticity theories and elasticity with the nonlocal and hall current parameters $\in = 0, \in = 0.03$ and $m = 0, m = 0.1$. In LEMV cylinders the frequency shift have linear nature for lower values of mode number and nonlinear nature for higher values of mode number in the presence and absence of nonlocal parameter. From the Figures 7 and 8, the discrepancy between frequency shift and mode number are observed in the presence of various thermoelasticity theories and elasticity with the nonlocal and hall current parameters $\in = 0, \in = 0.03$ and $m = 0, m = 0.1$ for thermoelastic hollow multilayered CFRP cylinders. In CFRP cylinders the frequency shift have experiences nonlinear nature for lower values of mode number and linear trend for higher values of mode number and he significant influence of nonlocal parameters has been observed.

Variation of thermoelastic damping against mode number of thermoelastic hollow multilayered LEMV/CFRP cylinders has been observed form Figures: 9–12 in the presence of various thermoelasticity theories and

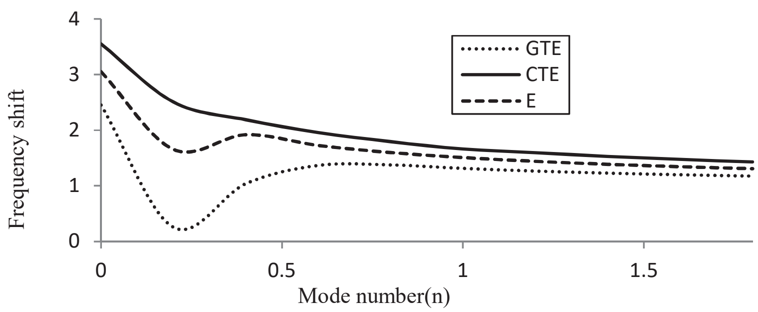

Figure 7 Variation of frequency shift against mode number (n) in the CFRP cylinder with $\in = 0.03$ & $m = 0.1$.

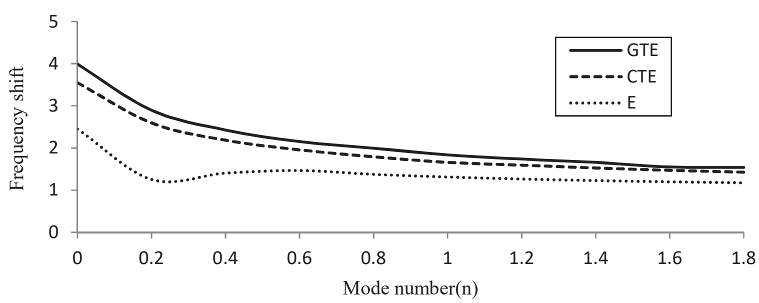

Figure 8 Variation of frequency shift against mode number (n) in the CFRP cylinder with $\in = 0$ & $m = 0$.

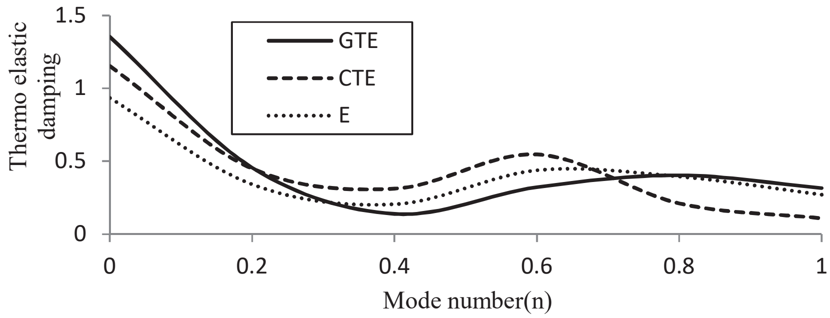

Figure 9 Variation of thermoelastic damping against mode number (n) in the LEMV cylinder with $\in = 0.03$ & $m = 0.1$.

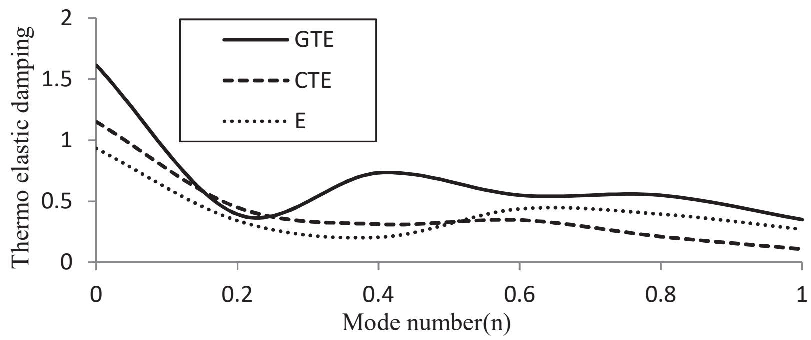

Figure 10 Variation of thermo elastic damping against mode number (n) in the LEMV cylinder with $\in = 0$ & $m = 0$.

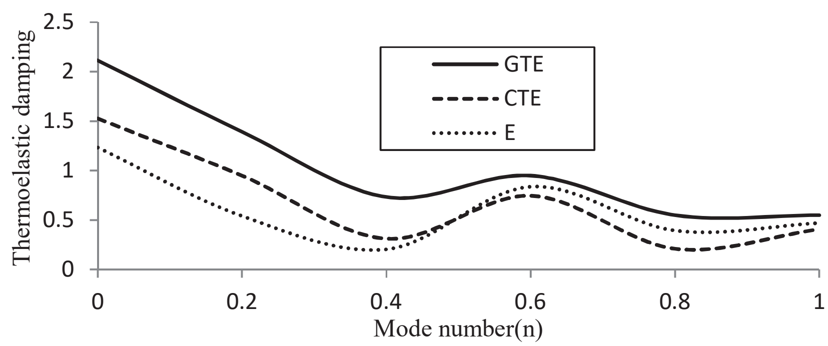

Figure 11 Variation of thermo elastic damping against mode number (n) in the CFRP cylinder with $\in = 0.03$ & $m = 0.1$.

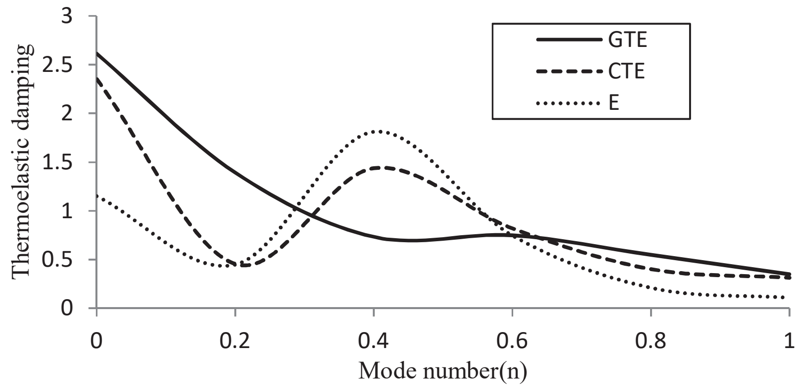

Figure 12 Variation of thermo elastic damping against mode number (n) in the CFRP cylinder with $\in = 0$ & $m = 0$.

elasticity with nonlocal and hall current parameters $\in = 0, \in = 0.03$ and $m = 0$, $m = 0.1$. In both LEMV/CFRP cylinders thermoelastic damping decreasing for lower values of mode number and retains oscillating nature for higher values of mode number. In both the cases, efficiency of the damping is increased by the nonlocal parameter.

7 Conclusions

This study proposed the natural frequency of a transversely isotropic nonlocal magneto thermoelastic multi-layered LEMV/CFRP hollow cylinder with Hall current. By using variable separation, governing equations can be converted into differential equations. The outer and inner surfaces of a hollow cylinder were determined to be stress free and thermally insulated/isothermal boundaries. According to the calculated analytical and numerical results, the influence of mode number on non-dimensional frequency, frequency shift, and thermoelastic damping is significantly affected by nonlocal parameter and phase lags of various thermoelasticity theories (GTE, CTE and E). Further, these improvements of mode number on the discussed physical variables were intensified by embedding CFRP core.

References

[1] A.C. Eringen, ‘Memory–dependent nonlocal electromagnetic elastic solids and super conductivity’, J Math Phys. 32, pp. 787–796, 1991.

[2] A.C. Eringen, 'Non-local Polar Field Models', Academic Press, New York.
[3] A.C. Eringen, 'Nonlocal Continuum Field Theories', Springer Verlag, New York, 2002.
[4] A.C. Eringen, 'Nonlocal polar elastic continua', Int. J. Eng. Sci., 10, pp. 1–16, 1972.
[5] A.C. Eringen, 'Theory of nonlocal thermoelasticity', Int. J. Eng. Sci., 1974.
[6] A.C. Eringen, 'On differential equations of nonlocal elasticity and solutions of screw dislocation and surface waves', J. Appl. Phys., 54, pp. 4703–4710, 1983.
[7] M. Davoodi, K. Zografos, P.J. Oliveira and R.J. Poole, 'On the similarities between the simplified Phan-Thien–Tanner model and the finitely extensible nonlinear elastic dumbbell [Peterlin closure] model in simple and complex flows', Phys. Fluids, 343, 033110, 2002.
[8] R. Hassani, R. Ansari, and H. Rouhi, 'An efficient numerical method to solve the problems of 2D incompressible nonlinear elasticity', Contin. Mech. Thermodyn., pp. 1–21, 2022.
[9] R.M. Chen, S. Walsh and M.H. Wheeler, 'Center manifolds without a phase space for quasilinear problems in elasticity, biology, and hydrodynamics', Nonlinearity, 35[4], 1927, 2022.
[10] Chen, H. Yang, K.I. Elkhodary, S. Tang and X. Guo, 'G-MAP123: A mechanistic-based data-driven approach for 3D nonlinear elastic modeling Via both uniaxial and equibiaxial tension experimental data', Extreme. Mech. Lett., 50, 101545 2022.
[11] L. Zubov and M. Karyakin, 'Nonlinear deformations of a cylindrical pipe with pre-stressed thin coatings', Mathematics and Mechanics of Solids, 2022.
[12] R. Selvamani, and S. Mahesh, 'Mathematical modeling and analysis of elastic waves in a thermo piezoelectric multilayered rotating composite rod with LEMV/CFRP interface', TechnischeMechanik-European Journal of Engineering Mechanics, 393, pp. 241–251, 2019.
[13] R. Selvamani, and S. Mahesh, 'Viscothermoelastic waves in a gravitated piezoelectric multilayered LEMV/CFRP cylinder coated with thin film', TechnischeMechanik-European Journal of Engineering Mechanics, 411, pp. 14–23, 2021.
[14] R. Selvamani, S. Mahesh, and F. Ebrahimi, 'Frequency characteristics of a multiferroic Piezoelectric/LEMV/CFRP/Piezomagnetic composite

hollow cylinder under the influence of rotation and hydrostatic stress', Coupled systems mechanics, 102, pp. 185–198, 2021.

[15] S. Mahesh, and R. Selvamani, 'Bending analysis of generalized thermoelastic waves in a multilayered cylinder using theory of dual phase lagging', J. Phys. Conf. Ser., 15971, 012013, 2020.

[16] W. Wagner and F. Gruttmann, ' On a Nonlinear Elastic Composite Shell Model with a Refined 3D Stress Analysis', In Current Trends and Open Problems in Computational Mechanics , Springer, pp. 553–567, 2022.

[17] C. D. Coman and A.P. Bassom, 'Axially compressed thin cylindrical shells: Asymptotic limits for a nonlinear basic state', International Journal of Non-Linear Mechanics, 138, 103848, 2022.

[18] H. Babaei, 'Thermomechanical analysis of snap-buckling phenomenon in long FG-CNTRC cylindrical panels resting on nonlinear elastic foundation', Composite Structures, 115199, 2022.

[19] S. Mondal and M. Kanoria, 'Thermoelastic solutions for thermal distributions moving over thin slim rod under memory-dependent three-phase lag magneto-thermoelasticity', Mech. Based Des. Struct, 483, pp. 277–298, 2020.

[20] S. Mondal, 'Memory response in a magneto-thermoelastic rod with moving heat source based on Eringen's nonlocal theory under dual-phase lag heat conduction', Int. J. Comput. Methods, 1709, 1950072, 2020.

[21] A. Alibeigloo, 'Three-dimensional thermoelasticity analysis of graphene platelets reinforced cylindrical panel', European Eur. J. Mech. A/Solids, 81, 103941, 2020.

[22] M. Bachher and N. Sarkar, ' Nonlocal theory of thermoelastic materials with voids and fractional derivative heat transfer', Waves in Random and Complex Media, 29[4], pp. 595–613, 2020.

[23] R. Kumar and R. Prasad, 'Thermoelastic interactions on hyperbolic two-temperature generalized thermoelasticity in an infinite medium with a cylindrical cavity', European. J. Mech. A/Solids, 82, 104007, 2020.

[24] E. Salari, and S.S. Vanini, 'Investigation of thermal preloading and porosity effects on the nonlocal nonlinear instability of FG nanobeams with geometrical imperfection', Eur. J. Mech. A/Solids, 86, 104183, 2021.

[25] P. Lata, S. Singh, 'Plane wave propagation in a nonlocal magneto-thermoelastic solid with two temperature and Hall current', Wave. Rand. Complex Media, pp. 1–27, 2020.

[26] P. Lata, S. Singh, 'Stoneley wave propagation in nonlocal isotropic magneto-thermoelastic solid with multi-dual-phase lag heat transfer', Steel Compos. Struct. 38,2, pp. 141–150, 2021.
[27] P. Lata, S. Singh, 'Effects due to two temperature and hall current in nonlocal isotropic magneto-thermoelastic solid with memory dependent derivatives', Coupled Systems Mechanics, 10,4, pp. 351–369, 2021.
[28] D. K. Sharma, H. Mittal, and S. R. Sharma, 'Forced vibration analysis in axisymmetric functionally graded viscothermoelastic hollow cylinder under dynamic pressure', Proceedings of the National Academy of Sciences, India Section A: Physical Sciences, 905, pp. 809–818, 2020.
[29] D. K. Sharma, M. K. Sharma., and N. Sarkar, 'Effect of three-phase-lag model on the analysis of three-dimensional free vibrations of viscothermoelastic solid cylinder,' Appl. Math. Model. 90, 281–301, 2021.
[30] D. K. Sharma, D. Thakur, and N. Sarkar, 'Effect of dual-phase-lag model on the vibration analysis of nonlocal generalized thermoelastic diffusive hollow sphere', Waves in Random and Complex Media, pp. 1–18, 2020.
[31] D.K. Sharma., D. Thakur., V. Walia,, and N. Sarkar, 'Free vibration analysis of a nonlocal thermoelastic hollow cylinder with diffusion', J. Therm. Stresses, 438, pp. 981–997, 2020.
[32] D. Sharma., P. C. Thakur, and N. Sarkar, 'Effect of dual-phase-lag model on free vibrations of isotropic homogenous nonlocal thermoelastic hollow sphere with voids', Mech. Based Des. Struct., pp. 1–17, 2020.
[33] N. Sharma, 'Analysis of free vibrations in transracially isotropic spherically symmetric thermoelastic spheres', Multidiscipline Modeling in Materials and Structures, 2020.
[34] A.M. Zenkour, 'Thermal-shock problem for a hollow cylinder via a multi-dual phase-lag theory', J. Therm. Stresses, pp. 687–706, 2020.
[35] V.K. Nelson, and S. Karthikeyan, 'Axisymmetric vibration of pyrocomposite hollow cylinder', World Academy of Science Engineering and Technology International Journal of Mathematical Computational Physical Electrical and Computer Engineering, 2008.

Biographies

Rajendran Selvamani is an Associate professor in the Department of Mathematics, Karunya University, Coimbatore, India. His research interests include solid mechanics, numerical methods, partial differential equations, and modelling of mechanical behaviours of nanomaterial. He has 20 years of teaching experience and has published more than 100 international research papers in reputed peer reviewed journals, and is the author of three books in well-known publishers.

S. Mahesh received the bachelor's degree in mathematics from Madurai Kamaraj University in 2009, the master's degree in mathematics from Bharathidasan University in 2011, and the philosophy of doctorate degree in mathematics from Karunya University in 2021, respectively. He is currently working as an Assistant Professor at the Department of Mathematics, V.S.B. Engineering College Karur, India. His research areas include Solid mechanics and thermodynamics.

Farzad Ebrahimi is an Associate Professor in the Department of Mechanical Engineering, IKIU, Qazvin, Iran. His research interests include mechanical behaviors of nano-engineered systems, mechanics of composites and nanocomposites, functionally graded materials, viscoelasticity, and smart materials and structures. Dr. Ebrahimi has authored more than 400 high-quality peer-reviewed research articles in his fields of interest. He has also edited and authored multiple books for well-known publishers. He is an Associate Editor of the journal Shock.